Supplementary information for Yield of reversible colloidal gels during flow startup: Release from kinetic arrest

Lilian C. Johnson, Benjamin J. Landrum, and Roseanna N. Zia

1 Rheology of $5kT$ gels

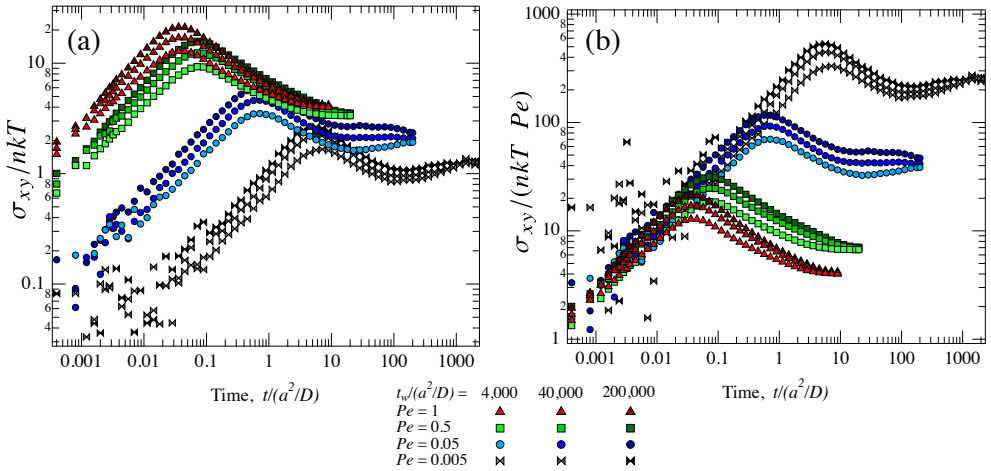

Figure S1: (a) Shear stress response scaled on the ideal osmotic pressure as a function of diffusively scaled time after startup for $5kT$ gels ranging in initial age from $4{,}000$ to $200{,}000a^2/D$ and flow strength $0.005 \leq Pe \leq 1$. (b) Shear stress response in plot (a) divided by the flow strength Pe of each curve.

The rheological response to startup shear for $5kT$ gels is shown in Figure S1. In Figure S1 (a), the $5kT$ gels exhibit a similar three-regime response in the shear stress σ_{xy} as a function of diffusive time $t/(a^2/D)$ after flow startup; this corresponds to the response shown for $6kT$ gels in Figure 4 (a) in §3.1.1. When the shear stress σ_{xy} is scaled on the Péclet number Pe, in Figure S1 (b), the $5kT$ gels exhibit the same collapse of the early-time stress growth within the same initial gel age (cf. Figure 4 (b) in §3.1.1 for the $6kT$ gels).

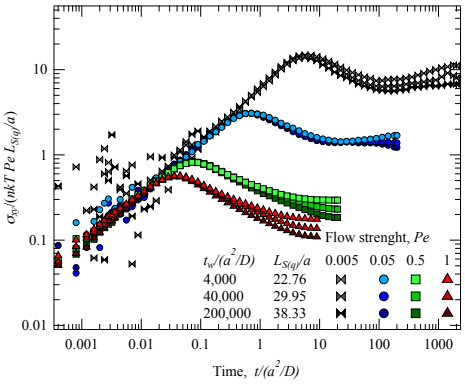

Figure S2: Shear stress scaled on both the flow strength and dominant length scale as a function of diffusive time for $5kT$ gels ranging in age from $4{,}000$ to $200{,}000a^2/D$. The dominant length scale, $L_{S(q)}/a$, used to scale each curve is shown in the legend (from Zia *et al.* [1]).

For $5kT$ gels, we scale the stress response upon the dominant length scale $L_{S(q)}$ from prior to startup in

Figure S2, as in Figure 5 in §3.1.1 for the $6kT$ gels. The collapse of the early-time behavior onto a single curve for all gels, regardless of age, also recovers the scaling we present in Equation 8.

2 Influence of bond strength on the pre-yield response

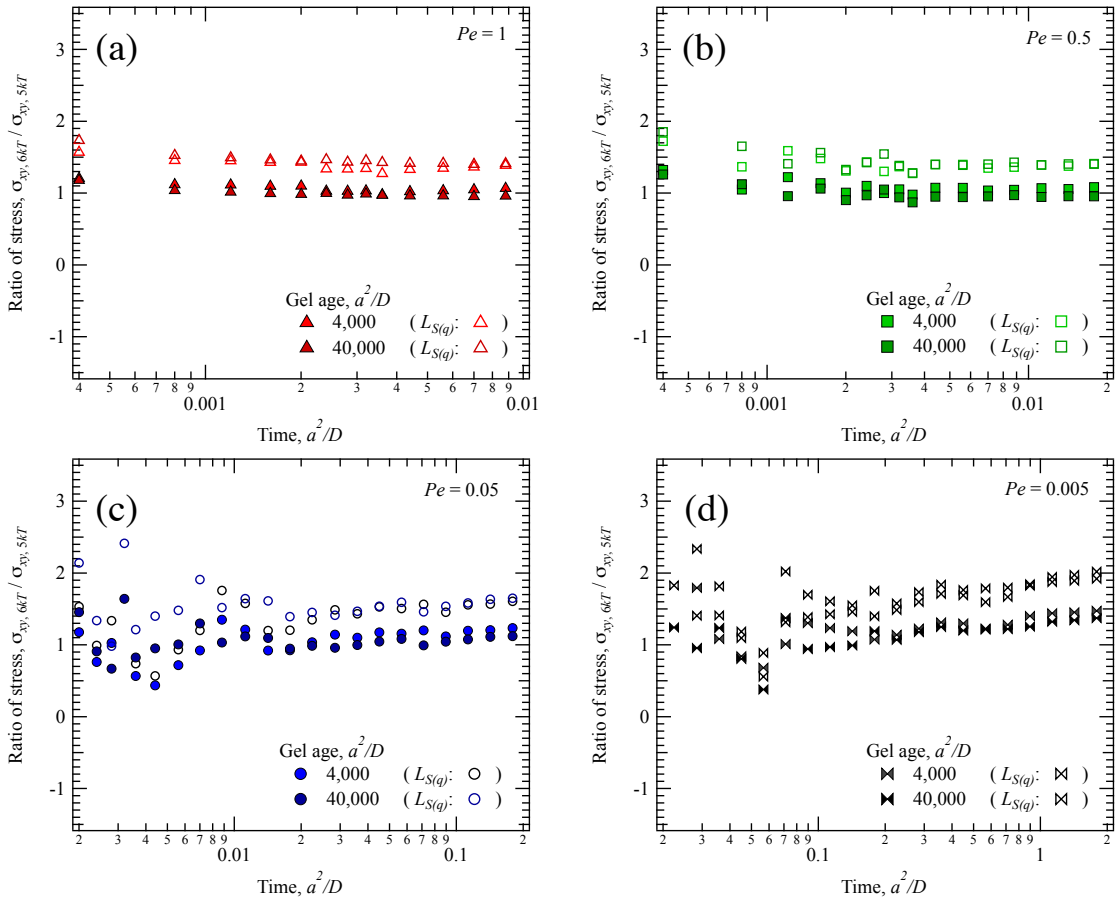

Figure S3: Pre-yield stress response of $6kT$ gels scaled on that of $5kT$ gels plotted as a function of diffusively scaled time after flow startup. The time range shown varies with flow strength to highlight the pre-yield regime. Closed/filled symbols represent the ratio of the stress response and open symbols represent the ratio of the stress response scaled on $L_{S(q)}$.

To examine the influence of bond strength on the pre-yield response, we scale the pre-yield stress of the $6kT$ gels on that of the $5kT$ gels at the same flow strength and age, Figures S3 (a)-(d). With stronger flow, Figure S3 (a)-(b), the rate of stress growth of the pre-yield response appears to be influenced little by changing the bond strength, but for weaker flow, Figures S3 (c)-(d), the bond strength appears to matter more, and the ratio of the stress increases at later times. When the ratio of the stress growth is also scaled by $L_{S(q)}$, the ratio becomes closer to 1.2, the ratio of 6 to 5, as flow strength increases. This ratio is consistent with the ratio of the high-frequency response of $6kT$ to $5kT$ gels in Zia et al. 2014.[1]

3 Influence of bond strength on the yield point

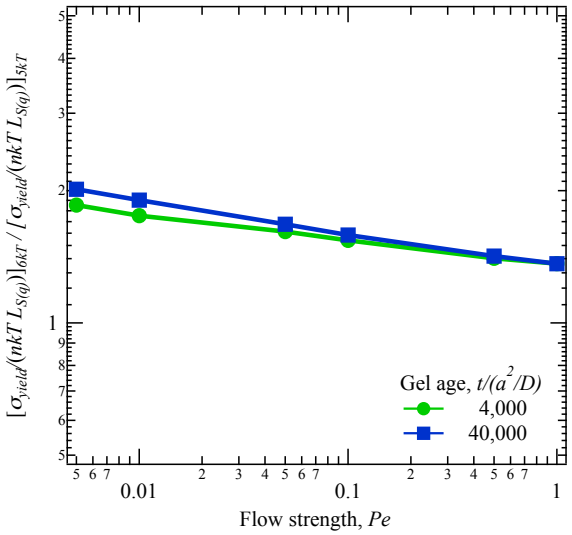

Figure S4: Ratio of yield stress (scaled on the ideal osmotic pressure and dominant length scale from prior to flow startup) of $6kT$ gels to that of $5kT$ gels as a function of flow strength, for gels of age 4,000 and 40,000 a^2/D.

To examine the role of the attraction strength on the yield stress, the ratio of $\sigma_{yield}/(nkT\,L_{S(q)})$ of the 6kT gels to the $5kT$ gels is plotted in Figure S4. The ratio of the yield stress of gels of different attraction strengths is greater than unity over the range of flow strengths examined. As flow strength increases, the ratio of the yield stresses approaches that of $6kT/5kT = 1.2$ which agrees with similar trends in frequency-dependent linear response: under weaker or less rapid perturbations, the steepness of the potential plays a bigger role as opposed to under stronger perturbations, where bond strength matters. Further, gel morphology plays a central role in the behavior of the gel and as such, simple scaling of the bond strength is not expected to remove the difference in behavior of gels of differing attraction strength.

4 Influence of age on bond dynamics and structure during startup

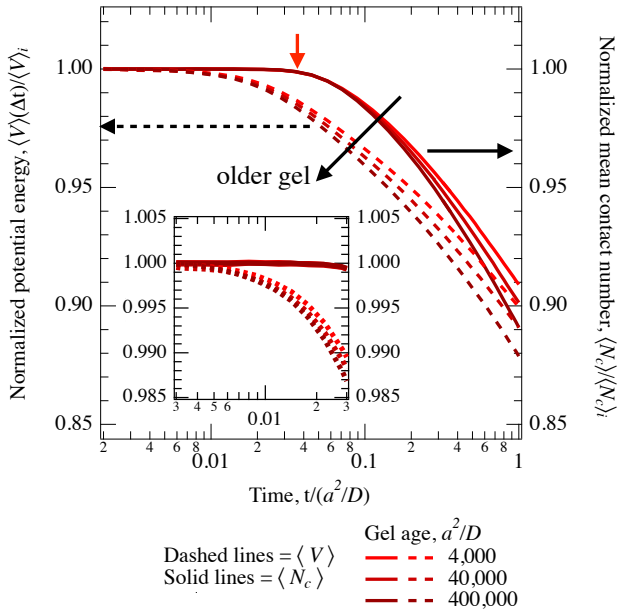

Figure S5: Bond dynamics: Normalized potential energy, left axis and dashed lines, and normalized mean contact number, right axis and solid lines, plotted as a function of diffusive time for $6kT$ gels with an initial age ranging from $4,000$ to $400,000a^2/D$ and flow strength $Pe = 1$. Colored vertical arrows indicate the yield point. Inset is the same figure, enlarged around the end of the pre-yield regime. Axes labels in insets are same as main plots.

Figure S5 shows the effect of gel age on bond dynamics. Again, the net number of bonds remains constant during the pre-yield regime, as evidenced by the constant value of $\langle N_c\rangle/\langle N_c\rangle_i$ (solid lines) until the yield point (marked by the colored vertical arrow). And as before, bond stretch, $\langle V\rangle/\langle V\rangle_i < 1$, plays a role in the late pre-yield regime and, here, becomes more pronounced with gel age. The increasing extent of bond stretching with advancing gel age suggests older gels exhibit disproportionally more bond stretching, and manifests as a greater rate of stress growth, Figure 4, as the increased number of bonds creates a greater resistance to flow. Because gels gain bonds continuously as they age, even proportional bond stretching should result in a greater rate of stress growth. However, one alternative explanation for disproportional bond stretching could lie in the role played by glassy dynamics and its influence on bond relaxation, that is, glassy dynamics holds bonds stretched.

The effect of initial gel age on flow-induced bond alignment is shown in Figure S6, where initially, at $t \ll 1$, age exerts no effect: the curves do not separate from one another during the pre-yield regime. That is, even though there may be pronounced difference in coarseness, the orientation of bonds during the pre-yield regime is not impacted by increasing the average number of bonds per particle. Differences in the orientation of bonds with gel age emerge at the yield point (marked by the colored vertical arrow) when net bond loss begins. We will recall that age influenced bond stretching during the late pre-yield regime (Figure S5). This age-dependent stretching suggest that age simply provides more bonds for flow to stretch, which corresponds to more particle cages in which store energy.

Bond dynamics, $\langle N_c\rangle/\langle N_c\rangle_i$ and $\langle V\rangle/\langle V\rangle_i$, are tracked as a function of strain for a $6kT$ gel at advancing ages for $Pe = 1$ in Figure S7 (a). A slight bond loss accompanies the yield point for each age, with gel age only exerting a weak influence on γ_{yield}. While the bond loss at yield does not vary with gel age, bond stretching does: the decrease below unity of $\langle V\rangle/\langle V\rangle_i$ (dashed curves) in Figure S7 (b), is more pronounced for older gels at the yield point. The normalization factor $\langle V\rangle_i$ increases in magnitude with gel age signifying a greater number of bonds, which indicates that older gels exhibit disproportionately more bond stretching. This disparity, or disproportional bond stretching, suggests that bond stretch is enhanced in older gels; as gel

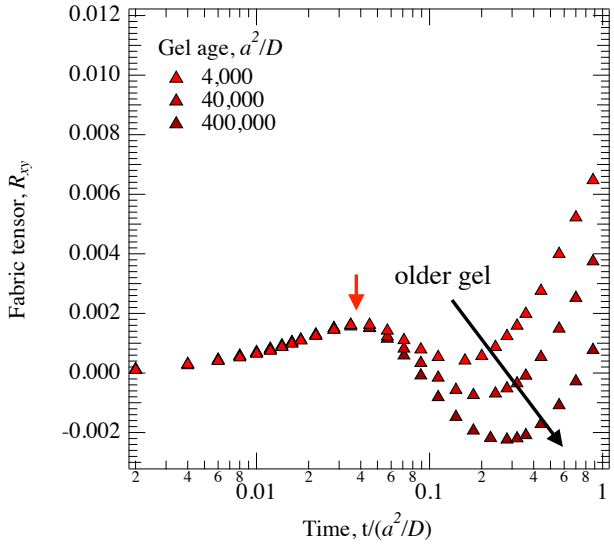

Figure S6: Orientation of bonds: Fabric tensor measured over the distance the attraction range ($\Delta = 0.1$) from each particle for a $6kT$ gel with an initial age varying from 400 to $400,000a^2/D$ and flow strength $Pe = 1$. Colored vertical arrows indicate the yield point.

age increases, particles acquire more bonds and further, glassy arrest deepens with age leading to reduced particle dynamics and increased steric hindrance.[1] In older gels, these features of glassy dynamics further slow the relaxation of bonds, prolonging bond stretch. That is, decreasing potential energy can be viewed not only as more bond stretch, but also as less bond relaxation.

Gel age has little impact on bond orientation at the yield point (Figure S8), in agreement with the near age-independence of the yield strain at this flow strength. It appears that entropic energy storage is nearly age-independent as advection grows, and the emergence of differences in energy storage primarily arises from the differences in bond stretching, explored earlier via $\langle V \rangle / \langle V_i \rangle$. Overall, this paints the picture that the rheological overshoot is set by an interplay of microscopic energy storage mechanisms: bond stretching and bond orientation. That is, bond orientation does not independently explain the rheological response.

Gel age influences the length scale of structure after the overshoot, comparing Figure S9 to Figure 19. Although the stress may begin to merge at long times for gels of different ages at $Pe = 1$ (Figure 4), we can clearly see that, for older gels, the structure following the overshoot (thick black dashed border) becomes aligned with flow retains the larger length scale from prior to flow. That is, bulk yielding does not necessarily erase the effects of age.

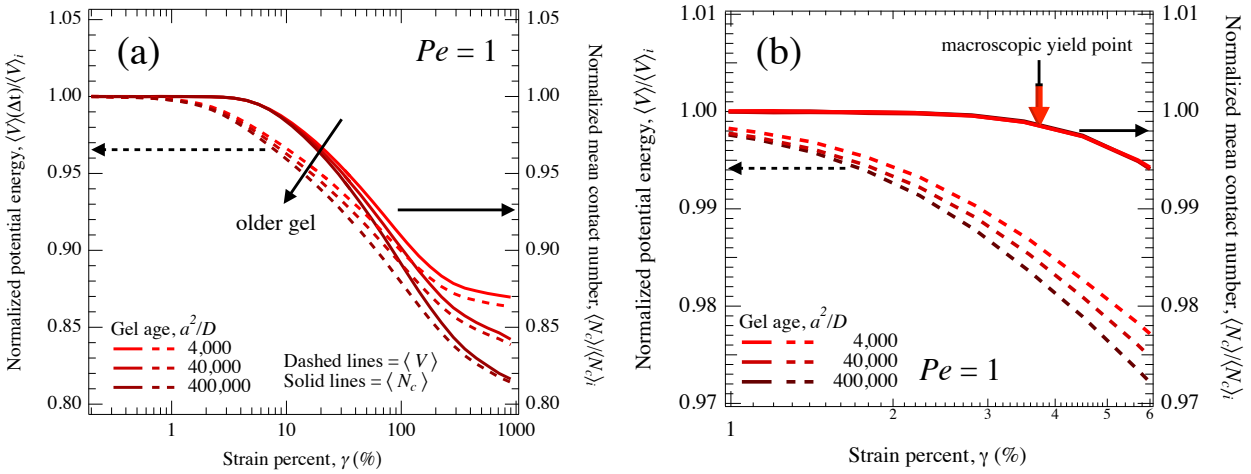

Figure S7: Bond dynamics: Normalized potential energy, left axis and dashed lines, and normalized mean contact number, right axis and solid lines, both plotted as a function of strain percent for a $6kT$ gel with initial age ranging from $4,000$ to $400,000a^2/D$ and flow strength $Pe = 1$. An enlarged view of (a) is shown in (b) with the yield point marked for each curve with an arrow of the corresponding color.

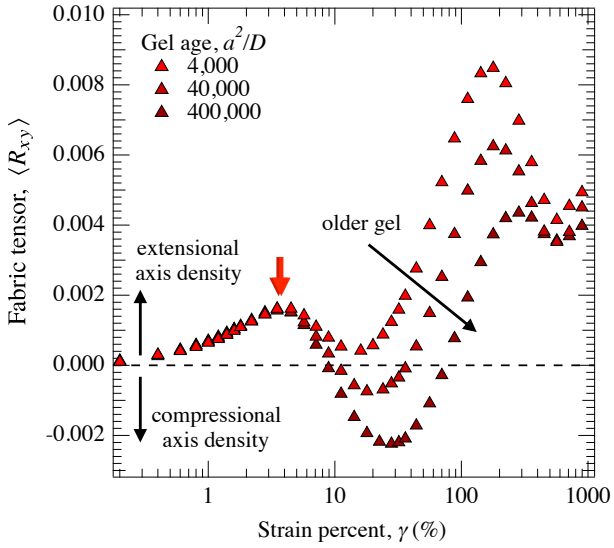

Figure S8: Orientation of bonds: Fabric tensor plotted as a function of strain percent for $6kT$ gels with initial age ranging from $4,000$ to $400,000a^2/D$ and flow strength $Pe = 1$. Colored arrows mark the yield point for the corresponding curve.

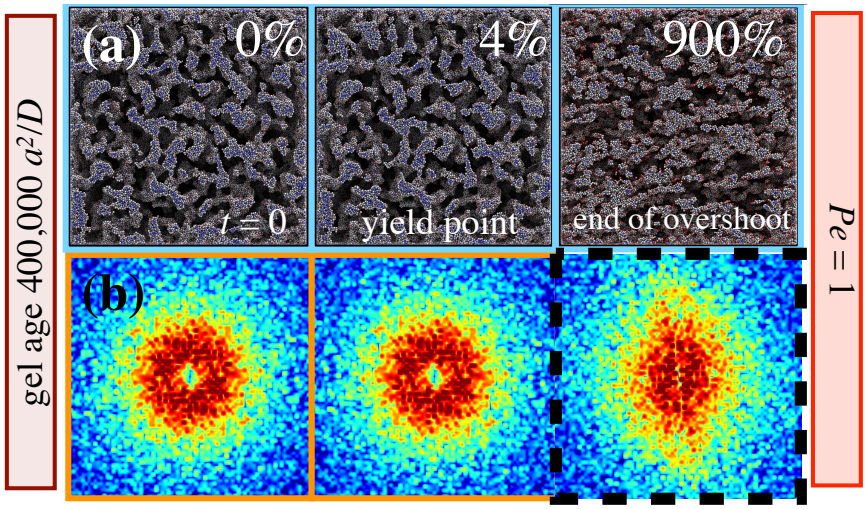

Figure S9: Evolution of structure under flow: Snapshots (a) and contour plots of the static structure factor $S(q)$ (b) of the flow-flow gradient plane at $\gamma = 0\%$, 4%, and the end of the overshoot or trough ($\gamma \sim 900\%$ shown) for $6kT$ gel of age $400,000a^2/D$ and flow strength $Pe = 1$. Snapshots are colored from red for particles with few contacts to blue for particles with many. Values of the contour plots range from 0.1 (blue) to 100 or greater (red).

5 Bond dynamics at the yield point for $5kT$ gels

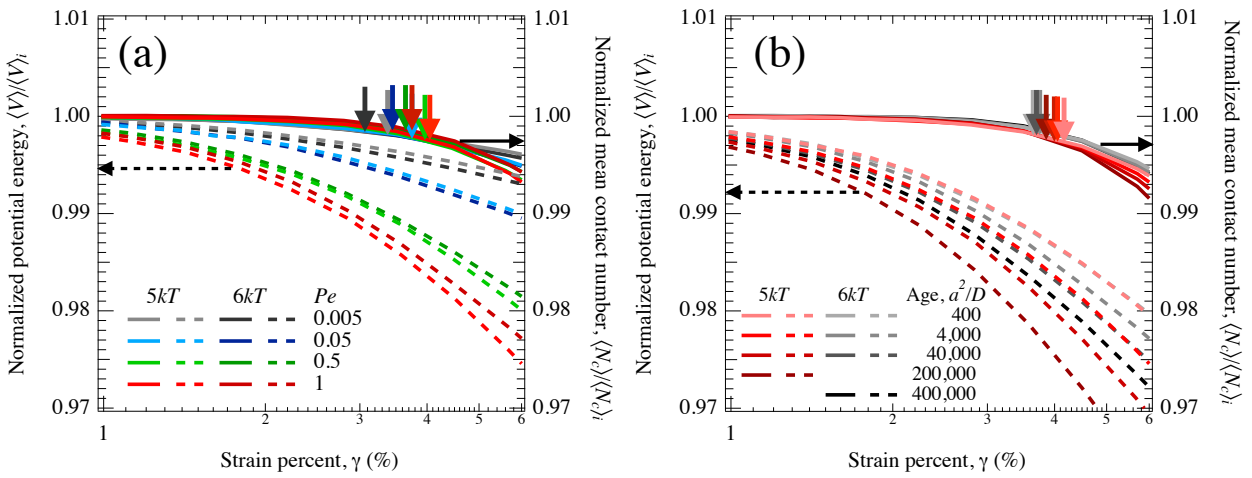

Figure S10: Macroscopic to microscopic comparison: Normalized potential energy $\langle V\rangle/\langle V\rangle_i$, left axis and dashed lines, and normalized mean contact number $\langle N_c\rangle/\langle N_c\rangle_i$, right axis and solid lines, both plotted as a function of strain, zoomed in around the yield point. (a) $5kT$ gels (lighter curves) and $6kT$ gels (darker curves) are shown at $0.005 \leq Pe \leq 1$ at age $4,000a^2/D$. (b) $5kT$ gels (red curves) and $6kT$ gels (grey curves) are shown for a range of ages under $Pe = 1$. Colored arrows mark the yield point for the corresponding curve.

We turn our attention to the micromechanical origins of the influence of stronger bonds on bulk yield. We observed that even with no change in attraction range, stronger bonds reduce bulk yield strain and reduce total work required to achieve yield (cf. Figure 14). Altering the bond strength, even from $6kT$ to $5kT$, alters both individual bond dynamics and gel coarseness. From the perspective of particle dynamics, each of the $5kT$ gels studied here is effectively "younger" than the corresponding $6kT$ gels at the same age, but the $5kT$ gels exhibit a greater $L_{S(q)}$ at each age due to more rapid coarsening.[1] $5kT$ gels require greater work at higher Pe than $6kT$ gels suggesting that the coarser large-scale structure requires more work to yield when flow is strong. As flow weakens, work required to yield merges for all gels, with the $6kT$ gels exhibiting a slightly higher work. This crossover in work required as the strength of imposed flow grows suggests again that the presence of elastic bonds matters when flow is weak, and coarser structure can further improve enthalpic energy storage as flow grows strong.

We also find the yield point in $5kT$ gels is set by a small net bond loss, Figures S10 (a) and (b). Stronger interparticle bonds lead to an earlier yield strain, given by arrows matching the darker curves for the $6kT$ gels, however, the bond loss observed at the yield point for the weaker $5kT$ gel (lighter solid curves) is greater than that of $6kT$ gels. That is, a net loss of approximately 0.20% of bonds accompanies the yield point for weaker $5kT$ gels, still less than tenths of a percent of the total number of bonds. We hypothesize that bond stretching is greater at stronger flow strengths for the $5kT$ gel as these bonds stretch with less force and bond breakage is greater at yield for weaker gels, also contributing to a decrease in the potential energy.

The role of interparticle attraction strength on the yield point can also be examined in light of its impact on the yield strain of progressively older gels. The impact of bond dynamics on the yield strain for $5kT$ (red curves) and $6kT$ (grey curves) gels of advancing age, subjected to $Pe = 1$, is shown in Figure S10 (b). The $6kT$ gel experiences both shorter yield strains (grey arrows) at the same flow strength and less variation in the yield strain at $Pe = 1$ than the $5kT$ gel (red arrows). The bond loss at the yield point is again greater for $5kT$ gels than $6kT$ gels, independent of gel age. Bond stretching (dashed curves) for $5kT$ and $6kT$ gels increases with gel age as found before. Glassy arrest in older gels hinders particle motion and slows progress towards a less-stretched configuration. Thus, glassy arrest enhances the bond stretch at the yield point as it prevents stretched bonds from relaxing.

We compare the response of $4,000a^2/D$ gels with $5kT$ bonds to $6kT$ bonds at various flow strengths in Figure S11 (a). $5kT$ gels (lighter markers) exhibit a reduced orientation of interparticle bonds at the yield

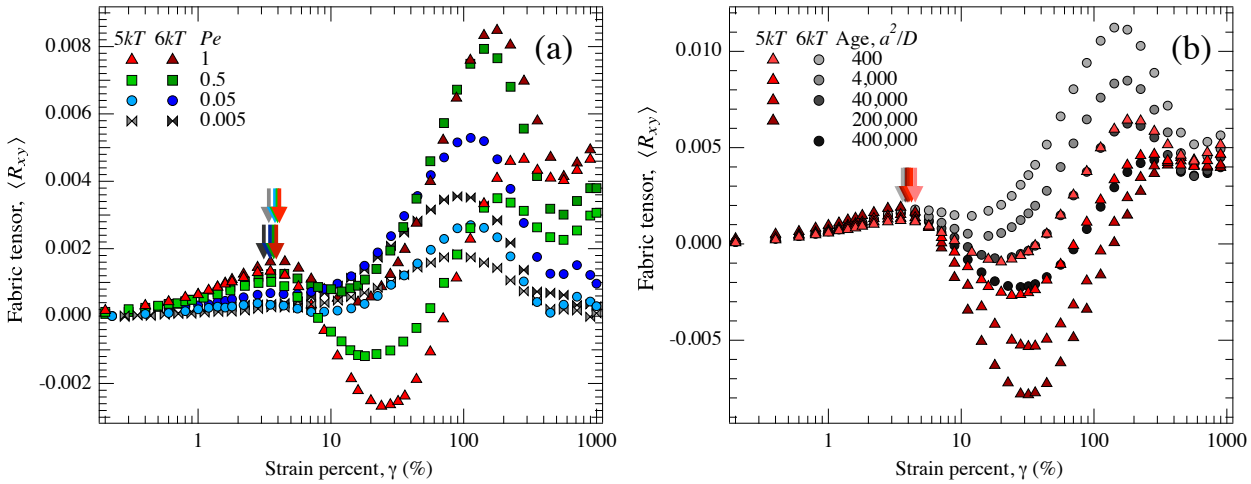

Figure S11: Orientation of bonds: Fabric tensor, for a distance of up to bond length ($\Delta = 0.1$) from each particle. (a) $5kT$ gels (lighter symbols) and $6kT$ gels (darker symbols) are shown at $0.005 \leq Pe \leq 1$ at age $4{,}000a^2/D$. (b) $5kT$ gels (red symbols) and $6kT$ gels (grey symbols) are shown for a range of ages under $Pe = 1$. Colored arrows mark the yield point for the corresponding curve.

point, and the yield point occurs slightly after the maximum in bond orientation rather than at the same moment as the yield point for stronger $6kT$ gels, and may be connected to the greater bond loss exhibited by $5kT$ gels. Interparticle bond strength also influences bond orientation at the yield point as a function of gel age, Figure S11 (b). Here, the fabric tensor is independent from the gel age up to the yield point for $6kT$ gels, but we see that $5kT$ gels exhibit an earlier age dependence.

References

[1] R. N. Zia, B. J. Landrum and W. B. Russel, *J. Rheol.*, 2014, **58**, 1121–1157.